



Effect of miR-4728-3p on the Regulation of PTEN in Apatinib-resistance SCLC Cell Line

Fang Chen

Department of Respiratory and Critical Care Medicine, Heping Hospital Affiliated to Changzhi Medical College, Changzhi, 046000, China

ABSTRACT

To explore the effects of microRNA (MicroRNA, miR)-4728-3p targeting regulation of phosphatase and TENsin homology deleted on chromosome 10 (PTEN) on the drug resistance of small cell lung cancer (SCLC) to apatinib. Human SCLC cell line H69 was purchased from the American Type Culture Collection. Through stepwise screening, an apatinib-resistant SCLC cell line (H69/Apatinib) was established. All cell lines were stored in RPMI-1640 medium, which was supplemented with 10% fetal bovine serum, 100 µg/ml streptomycin and 100 U/ml penicillin and kept in humid air containing 5% CO₂ at 37°C. The cell assay was performed when the cells were in the logarithmic growth phase. In the cultured H69/apatinib, the IC₅₀ of apatinib was greater than 30nM, while it was about 13µM in H69 parental cells (P<0.05), indicating that the anti-apatinib SCLC cells were successfully constructed *in vitro*. The expression of miR-4728-3p mRNA in the miR-4728-3p inhibitor group decreased, and the expression of PTEN mRNA increased (P<0.05). The miR-4728-3p mimic group showed no significant effect on the activity of mutant 3'UTR luciferase of PTEN (P>0.05). The miR-4728-3p inhibitor group had less cell migration and invasion, and its apoptosis rate increased (P<0.05). The abnormal expression of miR-4728-3p mediated the apatinib resistance of SCLC by targeting PTEN and regulating PI3 K/AKT pathway.

Article Information

Received 02 February 2021

Revised 06 March 2021

Accepted 18 March 2021

Available online 01 June 2022
(early access)

Published 10 April 2023

Key words

miR-4728-3p, PTEN, Small cell lung cancer, Apatinib, Drug resistance.

INTRODUCTION

Lung cancer has become the main cause of cancer-related deaths all over the world. Among it, small cell lung cancer (SCLC) accounts for 14%, with a 5-year mortality rate of about 90%. SCLC is highly invasive and has great metastasis potential (Chai *et al.*, 2020). It has been suggested that radiotherapy combined with thoracic and mediastinum can improve the 3-year survival rate from 8.9% to 14.3% in patients with limited SCLC (Guo *et al.*, 2020). However, despite the initial treatment response, most SCLC patients can still tolerate chemotherapy and radiotherapy. Therefore, it is urgent to explore new target therapies to overcome multidrug resistance and radiation resistance (Wang *et al.*, 2020). miRNA is a series of endogenous small non-coding RNA with a length of about 22 nucleotides, playing a key role in regulating cell proliferation, differentiation, apoptosis, migration and

invasion through mRNA instability and translation inhibition in various human tumors (Liu *et al.*, 2019). Our previous studies have identified 61 miRNAs based on miRNA array analysis. They are differentially expressed between multidrug-resistant SCLC cells and parental H69 cells (Huang *et al.*, 2019). According to reports, miR-4728-3p can promote the progression of various cancer types, including breast cancer and hepatocellular carcinoma (Liu *et al.*, 2020). In SCLC, the increase of miR-4728-3p expression level is related to brain metastasis (Wang and Du., 2020). However, the role of miR-4728-3p in the development of apatinib resistance in SCLC is still unclear. Phosphatase and TENsin homology deleted on chromosome 10 (PTEN), located on human chromosome 10q23, is a tumor suppressor gene and an inhibitor of PI3 K/Akt pathway (Xiong *et al.*, 2020). Although the mechanism of PTEN mutation and loss of expression is not fully understood, the decrease of PTEN expression level and mutation are usually observed in lung cancer. In addition, studies have shown that PTEN is mediated by many miRNA. The expression of miRNA-492 promotes the progression of liver cancer by targeting PTEN (Li *et al.*, 2020). miRNA-221 and miRNA-222 regulate the proliferation and radioresistance of gastric cancer cells by targeting PTEN. In addition, studies have shown that miR-21 and miR-26a regulate the expression of PTEN in SCLC

* Corresponding author: chenfang19810904@163.com
0030-9923/2023/0003-1333 \$ 9.00/0



Copyright 2023 by the authors. Licensee Zoological Society of Pakistan.

This article is an open access article distributed under the terms and conditions of the Creative Commons Attribution (CC BY) license (<https://creativecommons.org/licenses/by/4.0/>).

(Li *et al.*, 2019). However, it is not clear whether PTEN is directly related to miR-4728-3p in SCLC. Therefore, we studied the effects of targeted regulation of PTEN by miR-4728-3p on apatinib-resistant SCLC.

MATERIALS AND METHODS

Cell line and cell culture

Human SCLC cell line H69 was purchased from American Type Culture Collection (ATCC). The apatinib-resistant SCLC cell line (H69/apatinib) was established by increasing the concentration of apatinib to 30-60nM through six-month culture. Apatinib resistance was maintained with 30 nM apatinib in culture. All cell lines were stored in RPMI-1640 medium supplemented with 10% fetal bovine serum (Invitrogen, Carlsbad, CA, USA), 100 g/ml streptomycin and 100 U/ml penicillin (Sigma-Aldrich, St. Louis, Missouri, USA) in humid air containing 5% CO₂ at 37°C. Cell assay was performed when cells were in the logarithmic growth phase.

Cell transfection

Cell transfection was carried out on cells in the logarithmic growth phase. Transient cell transfection of miR-4728-3p mimic, miR-4728-3p inhibitor and NC control (Invitrogen) was carried out using Lipofectamine™ 3000 transfection reagent (Thermo Fisher Scientific, Waltham, Massachusetts, USA). After transfection for 12 h, fresh medium was added to the plate for cell culture. Sequence of miR-4728-3p mimic is 5'-GACAUCAGACACUACCUG-3'.

RNA isolation and quantitative real-time PCR

Total RNA was extracted with Trizol reagent (Invitrogen, USA) according to the manufacturer's instructions. To analyze gene expression, real-time RT-PCR was performed on a real-time PCR instrument using SYBR®PrimeScript™RT-PCR kit (Takara Biotechnology, China). The relative quantitative PCR conditions include: initial denaturation at 95°C for 30s, denaturation at 95°C for 5s and 60°C for 30s for 40 cycles, denaturation at 95°C for 15s, and denaturation at 55°C for 45s and 95°C for 15s. The relative expression of miRNA and its glyceraldehyde-3-phosphate dehydrogenase (GAPDH) of mRNA were normalized to U6 by 2^{-ΔΔCt}. All reactions were tested in at least triplicate.

Dual luciferase reporter gene detection

Wild-type PTEN 3' untranslated region (UTR) and miR-4728-3p binding site on mutant PTEN 3'-UTR were inserted into pGL3 reporter luciferase reporter vector (Sigma-Aldrich, St. Louis, Missouri, USA). According

to the manufacturer's instructions, miR-4728-3p mimic and control miRNA were co-transfected into cells with pGL3-3'-UTR wild-type or mutant plasmid DNA through Lipofectamine 3000. Twenty-four hours after transfection, the relative luciferase activity was analyzed by dual luciferase reporter gene analysis system (Promega, Madison, Wisconsin, USA), and standardization was carried out by Renilla luciferase reference plasmid.

CCK-8 assay

Quantitative cell viability was evaluated by cell counting kit 8 (CCK-8). Cells used for experiments were inoculated into wells of a 96-well plate (1×10⁴ cells per well) and kept overnight to adhere the cells. After transfection for a certain time (24 h, 48 h and 72 h), 20μl CCK-8 solution (Sigma Chemicals, St. Louis, Missouri, USA) was added to each well, and the cells were incubated for 10 min. After another 4 h, the absorbance (optical density) value was measured at a wavelength of 450 nm using an enzyme-linked immunosorbent assay (MultiskanEX, Lab Systems, Helsinki, Finland).

Transwell analysis

Transfected H69/apatinib cells were evaluated by Transwell assay to determine migration and invasion ability. Transfected cells were placed in a 24-well cross-well chamber (8μm well; corning). Transfected cells (2×10⁴ cells/ml) were re-suspended in 200 μl serum-free medium, and laid in the upper chamber, and the lower chamber was filled with 500μL complete medium containing 10%FBS. After incubation at 37°C for 24 h, the cells on the lower surface were stained with 0.1% crystal violet at room temperature for 15 min, and then photographed and counted under an optical microscope.

Flow cytometry analysis

Cells were collected, washed and resuspended in phosphate buffer (PBS), and stained with Annexin V and propidium iodide (PI) using Annexin V-FITC/PI apoptosis detection kit (BD Biosciences, San Jose, California, USA). According to the manufacturer's agreement, the percentage of apoptotic cells was determined by FACS Calibur flow cytometry (BD Biosciences). FlowJo 6.0 software was used for data analysis. This process was repeated three times.

Western blot analysis

Cells were lysed with cold RIPA lysis buffer, and protein concentration assay was performed by standard BCA method (BCA protein assay kit, USA). The same amount of protein was loaded and separated by 10% SDS-PAGE. Protein was then transferred to polyvinylidene

fluoride (PVDF) membrane (Millipore, USA). After sealing with 5% fat-free milk for 2 h, the membrane was incubated with specific PI3K (Abcam), Akt (Abcam) and β -actin (Jackson) antibodies at 4°C overnight. After washing, the membrane was incubated with horseradish peroxidase labeled secondary antibody for 1 h at room temperature. Immunoblot was detected by enhanced chemiluminescence system (Beyotime, China). β -actin was used as a control in this assay. Image-Pro Plus 6.0 software was used for protein quantitative analysis.

Statistical analysis

All experiments were repeated 3 times, and all statistical analyses were performed using GraphPad Prism 5.0 (GraphPad Software, Inc., La Jolla, CA, USA). All data were expressed as mean \pm standard deviation. Pearson correlation analysis was used for correlation analysis. The differences between the two groups were compared by student t-test. The differences between the two groups were analyzed by one-way ANOVA and Newman-Kiel analysis was performed. $P < 0.05$ indicated statistically significant difference.

RESULTS AND DISCUSSION

The IC_{50} of drug-resistant H69/apatinib cells was higher

The cultured h69/apatinib cells were identified by analyzing the inhibitory concentration (IC_{50}) of 50% apatinib. The results showed that the IC_{50} of apatinib in cultured H69/apatinib was greater than 30nM, while it was about 13 μ m in H69 parent cells ($P < 0.05$), which indicated that anti-apatinib SCLC cells were successfully prepared *in vitro* (Table I).

Table I.- Comparison of IC_{50} between two groups.

Group	IC_{50} (nM)
H69 group	13.15 \pm 1.26
H69/apatinib group	35.43 \pm 1.58
<i>t</i> value	8.927
<i>P</i> value	0.013

Table II.- Effect of apatinib induced resistance on expression of mir-4728-3p and PTEN in SCLC cells.

Group	H69	H69/apatinib	<i>t</i>	<i>P</i>
miR-4728-3p	3.55 \pm 0.27	6.42 \pm 0.18	6.927	0.014
PTEN	2.38 \pm 0.24	0.56 \pm 0.13	8.967	0.012

The expression of miR-4728-3p in drug-resistant H69/apatinib cells was higher

To study the effect of miR-4728-3p on apatinib

resistance in SCLC, qRT-PCR was used to analyze the expression level of miR-4728-3p and PTEN mRNA. Compared with the apatinib-sensitive H69 group, the mRNA expression of miR-4728-3p increased and that of PTEN decreased in apatinib-resistant H69/Apatinib group ($P < 0.05$) (Fig. 1, Table II).

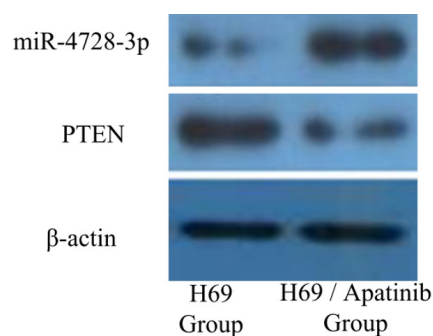


Fig. 1. qRT-PCR analysis of expression levels of miR-4728-3p and PTEN mRNA.

miR-4728-3p regulated PTEN expression

To further explore the role of miR-4728-3p, SCLC cells were treated with miR-4728-3p mimics, miR-4728-3p inhibitors and their control, respectively. Compared with the control group, the mRNA expression of miR-4728-3p increased and the mRNA expression of PTEN decreased ($P < 0.05$) in the miR-4728-3p mimic group. The mRNA expression of miR-4728-3p in the miR-4728-3p inhibitor group decreased, while the mRNA expression of PTEN increased ($P < 0.05$) (Table III).

Table III.- mRNA expression levels of mir-4728-3p and PTEN.

Group	Control	miR-4728-3p mimic	miR-4728-3p inhibitor	<i>t</i>	<i>P</i>
miR-4728-3p	6.43 \pm 0.35	12.38 \pm 1.87	2.24 \pm 0.28	12.36	0.012
PTEN	0.84 \pm 0.33	0.15 \pm 0.06	3.78 \pm 0.14	12.32	<0.001

Table IV.- Luciferase assay.

Group	Control	miR-4728-3p mimic	<i>t</i>	<i>P</i>
Wild-type	613.82 \pm 11.46	237.57 \pm 15.47	12.738	0.015
Mutant-type	576.82 \pm 25.81	568.91 \pm 22.13	15.726	0.013

Dual luciferase assay of targeted regulation of PTEN by miR-4728-3p

To further explore the mechanism of miR-4728-3p regulating the sensitivity of drug-resistant SCLC cells to apatinib, the potential target genes of miR-4728-3p were

analyzed by bioinformatics analysis (microRNA.org/miRWalk). PTEN contains a binding region complementary to miR-4728-3p in 3'-UTR. The results of dual luciferase reporter gene analysis showed that compared with the control group, the wild-type 3'-UTR co-transfected cells of PTEN in miR-4728-3p mimic group showed lower luciferase activity ($P<0.05$). The miR-4728-3p mimic group showed no significant effect on the activity of mutant 3'UTR luciferase of PTEN ($P>0.05$). The results indicated that miR-4728-3p could affect apatinib resistance of SCLC by targeting PTEN (Table IV).

miR-4728-3p regulated the survival of SCLC cells

The viability of SCLC cells in different treatment groups was analyzed by CCK-8. Compared with the control group, the viability of miR-4728-3p mimic group increased at 24 h, 48 h and 72 h ($P<0.05$), while the viability of miR-4728-3p inhibitor group decreased at 4 h, 48 h and 72 h ($P<0.05$) (Table V).

miR-4728-3p regulated migration, invasion and apoptosis of SCLC cells

Transwell was used to analyze the migration and invasion ability of cells, and FACS Calibur flow cytometry was used to determine the percentage of apoptotic cells. Compared with the control group, the cell migration and

invasion of miR-4728-3p mimic group increased and its cell apoptosis rate decreased ($P<0.05$), while the cell migration and invasion of miR-4728-3p inhibitor group cells decreased and its cell apoptosis rate increased ($P<0.05$) (Fig. 2; Table VI).

Table V.- Cell viability (OD value).

Group	0h	24h	48h	72h
Control group	0.25±0.05	0.63±0.08	0.82±0.09	1.46±0.32
miR-4728-3p mimic group	0.25±0.06	0.88±0.53	1.23±0.15	1.93±0.16
miR-4728-3p inhibitor group	0.25±0.07	0.34±0.15	0.54±0.09	0.87±0.11
<i>t</i> value	16.9276	17.927	17.826	13.917
<i>P</i> value	0.816	0.007	<0.001	<0.001

miR-4728-3p regulated PI3K/Akt signaling pathway

The expression levels of PI3K and Akt protein were analyzed by western blot. Compared with the control group, the expression levels of PI3K and Akt proteins in the miR-4728-3p mimic group increased ($P<0.05$), while the expression levels of PI3K and Akt proteins in the miR-4728-3p inhibitor group decreased ($P<0.05$) (Table VII).

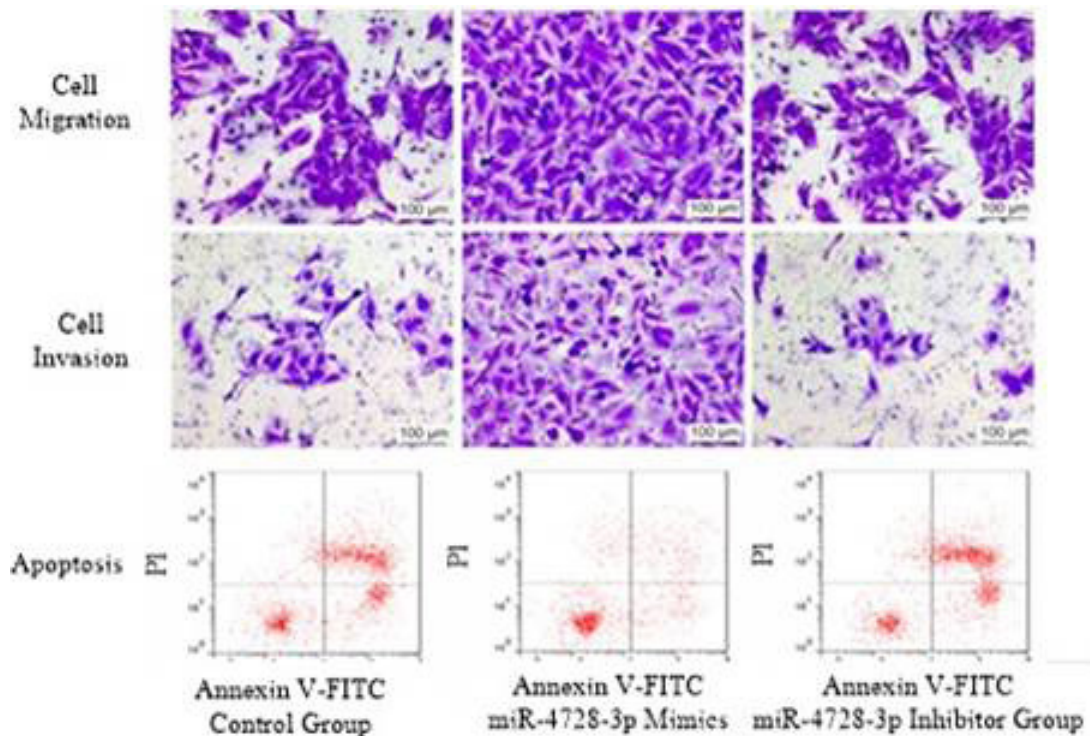


Fig. 2. Detection of cell migration, invasion and apoptosis of miR-4728-3p mimic group compared with the control group.

Table VI.- Rate of cell migration, invasion and apoptosis.

Group	Migration rate (%)	Invasion rate (%)	Apoptosis rate (%)
Control group	68.82±2.78	43.72±4.72	18.98±1.63
miR-4728-3p mimic group	98.63±1.54	98.67±6.33	6.87±0.23
miR-4728-3p inhibitor group	44.88±2.76	25.78±3.72	43.45±2.23
<i>t</i> value	13.826	14.829	15.728
<i>P</i> value	0.014	0.013	0.015

Table VII.- Expression levels of PI3K and Akt protein.

Group	PI3K	Akt
Control group	1.58±0.13	2.75±0.33
miR-4728-3p mimic group	6.47±0.25	8.46±0.14
miR-4728-3p inhibitor group	0.34±0.16	1.03±0.12
<i>t</i> value	11.182	13.547
<i>P</i> value	0.004	0.002

DISCUSSION

Regardless of the increasing studies on SCLC, no obvious treatment progress has been made, and chemotherapy and radiotherapy are still the main treatment methods (Chen *et al.*, 2019). Although SCLC is sensitive to the initial chemoradiation therapy, most SCLC patients will eventually develop chemoradiation resistance, and will not benefit from the current therapy eventually. Therefore, how to reverse chemical or radiation resistance and improve the therapeutic effect remains a key issue.

miRNA is a group of endogenous small non-coding RNA with a length of about 22 nucleotides. Functionally, miRNA participates in many cellular processes, including proliferation, apoptosis, migration (Pang *et al.*, 2020). In addition, it is well known that miRNA is an important regulator of various pathophysiological processes and drug resistance in carcinogenesis. More and more evidences show that miRNA is involved in a variety of cellular functions and plays an oncogene or cancer suppression role (Chen *et al.*, 2013). Studies have shown that miRNAs may be a new biomarker, and may even become a potential target in cancer treatment. For example, miRNA, including miR-10a, miR-26, miR-30c, miR-126a, miR-210, miR-342 and miR-519a, play a role in tamoxifen resistance in breast cancer patients (Yin *et al.*, 2019). miRNA may also be involved in multidrug resistance of gastric cancer.

miR-210 enhances the radiation resistance of human lung cancer cell A549 by promoting hypoxia (Hao *et al.*, 2020). In our research, miR-4728-3p was selected based on our previous miRNA array analysis. At first, the expression of miR-4728-3p in SCLC cell line was analyzed by qRT-PCR. Compared with the parent cell line, the expression of miR-4728-3p in SCLC drug-resistant cells H69/apatinib increased.

Recent studies have reported that miR-4728-3p plays a role in inhibiting cancer in various malignant tumors. In SCLC, miR-4728-3p has been proved to have low expression and is involved in the tumorigenesis, development and prognosis. In addition, more and more evidence shows that miR-4728-3p is associated with chemical resistance and is related to several chemotherapeutic drugs, such as paclitaxel, methotrexate, platinum and cisplatin (Li *et al.*, 2019). In SCLC, miR-4728-3p was announced to regulate paclitaxel resistance of SCLC cells *in vivo* and *in vitro*. However, its role in regulating apatinib resistance has not been studied in SCLC. PTEN is a recognized phosphatase and a tumor suppressor, which may mutate in various cancers (Nuzzo *et al.*, 2019). PTEN exerts its anti-cancer effect by negatively regulating PI3K/AKT signaling pathway (Tang *et al.*, 2019). The expression of PTEN is strictly controlled by non-coding RNA, protein-protein interaction and protein modification. The change of PTEN expression or activity may lead to uncontrolled activation of PI3K-AKT signaling pathway, which may promote cancer progression and induce drug resistance (Li *et al.*, 2017). To explore the mechanism of miR-4728-3p regulating apatinib resistance of SCLC, we predicted the target gene of miR-4728-3p by bioinformatics analysis. Our experimental results showed that miR-4728-3p directly bound to the 3'-UTR of PTEN. We found that down-regulation of miR-4728-3p expression could promote apoptosis and inhibit cell migration in H69/apatinib cells. We also observed that miR-4728-3p was negatively correlated with PTEN in SCLC *in vivo* and *in vitro*. PTEN was expressed at low level in SCLC, and its down-regulation was related to accelerating lung cancer growth and increasing invasion. MiR-4728-3p could change the expression level of PTEN and activate PI3K/Akt signaling pathway, thus playing a role in apatinib resistance in SCLC. However, our current findings deserve further study, and the role of other miRNAs in apatinib resistance also need further study.

In summary, abnormal expression of miR-4728-3p mediated the apatinib resistance of SCLC by targeting PTEN to regulate the PI3K/AKT pathway.

Statement of conflict of interest

The authors have declared no conflict of interests.

REFERENCES

- Chai, J., Wang, Y.Y., Zhang, J.Y., Niu, Q., Hu, Y.H., Li, Y., Wang, H.X. and Li, S.G., 2020. Meta-analysis of multiple regulatory effects of arsenic on PI3K/AKT signaling pathway. *J. environ. Hyg.*, **10**: 31-37.
- Chen, G., Yu, L., Dong, H., Liu, Z. and Sun, Y., 2019. miR-182 enhances radioresistance in non-small cell lung cancer cells by regulating FOXO 3. *Clin. exp. Pharmacol. Physiol.*, **46**: 137-143. <https://doi.org/10.1111/1440-1681.13041>
- Chen, Y., Liang, J.G. and Zhang, W.D., 2013. New progress in screening biomarkers of EGFR-TKI for non-small cell lung cancer. *J. Pract. Med.*, **29**: 1035-1036.
- Guo, Y.N., Jiang, B., Guo, H.Y., Wang, T., Zhang, Y.D. and Su, H.X., 2020. Research progress of drug resistance mechanism and reversal of drug resistance in non-small cell lung cancer. *Gansu med. J.*, **39**: 871-875.
- Hao, J.H., Cheng, J., Cheng, R. and Zhong, J., 2020. Correlation between miR-218 and cisplatin resistance in oral cancer. *Genom. appl. Biol.*, **39**: 1830-1836.
- Huang, G., Lou, T., Pan, J., Ye, Z., Yin, Z., Li, L., Cheng, W. and Cao, Z., 2019. MiR-204 reduces cisplatin resistance in non-small cell lung cancer through suppression of the caveolin-1/AKT/Bad pathway. *Aging*, **11**: 2138. <https://doi.org/10.18632/aging.101907>
- Huanhuan, L., Zhidan, D., Dongfeng, Y., Jie, M. and Jianjun, Q., 2016. Diagnostic value of folate receptor-positive circulating tumor cell in lung cancer: A pilot study. *Zhongguo Fei Ai Za Zhi*, **19**: 813-820.
- Li, D., Zhou, W., Gao, X.B., Wang, X.X., Guo, S., Shi, L. and Zhang, S., 2019. Matrine inhibits Nrf2 induced annexin A4 expression and improves cisplatin resistance in non-small cell lung cancer. *Int. J. Pathol. clin. Med.*, **39**: 457-463.
- Li, G., Wang, J.S., Qin, S.D., Sun, X., Ren, H., Zhang, J. and Li, B.C., 2019. Application of detection of circulating tumor cells and exosome miR-21 in diagnosis of lung ground glass opacity. *J. Jilin Univ. (Med. Ed.)*, **45**: 587-594.
- Li, L., Li, B., Xin, H.Y. and Chen, J.H., 2017. Study on the relationship between cisplatin-resistance of human ovarian cancer cell and TLR9 under hypoxia. *China Pharm.*, **28**: 1744-1747.
- Li, Z., Qu, Z., Wang, Y., Qin, M. and Zhang, H., 2020. miR-101-3p sensitizes non-small cell lung cancer cells to irradiation. *Open Med.*, **15**: 413-423. <https://doi.org/10.1515/med-2020-0044>
- Liu, X., Zhou, X., Chen, Y., Huang, Y., He, J. and Luo, H., 2019. miR-186-5p targeting SIX1 inhibits cisplatin resistance in non-small-cell lung cancer cells (NSCLCs). *Neoplasma*, **67**: 147-157. https://doi.org/10.4149/neo_2019_190511N420
- Liu, Z., Guo, Z., Long, L., Zhang, Y., Lu, Y., Wu, D. and Dong, Z., 2020. Spindle assembly checkpoint complex-related genes TTK and MAD2L1 are over-expressed in lung adenocarcinoma: a big data and bioinformatics analysis. *J. S. med. Univ.*, **40**: 1422-1431.
- Nuzzo, S., Catuogno, S., Capuozzo, M., Fiorelli, A., Swiderski, P., Boccella, S., de Nigris, F. and Esposito, C.L., 2019. Axl-targeted delivery of the oncosuppressor miR-137 in non-small-cell lung cancer. *Mol. Ther. Nucl. Acids*, **17**: 256-263. <https://doi.org/10.1016/j.omtn.2019.06.002>
- Pang, J., Ye, L., Zhao, D., Zhao, D. and Chen, Q., 2020. Circular RNA PRMT5 confers cisplatin-resistance via miR-4458/REV3L axis in non-small-cell lung cancer. *Cell Biol. Int.*, **44**: 2416-2426. <https://doi.org/10.1002/cbin.11449>
- Tang, X., Jiang, J., Zhu, J., He, N. and Tan, J., 2019. HOXA4-regulated miR-138 suppresses proliferation and gefitinib resistance in non-small cell lung cancer. *Mol. Genet. Genom.*, **294**: 85-93. <https://doi.org/10.1007/s00438-018-1489-3>
- Wang, Q., Chen, Y., Lu, H., Wang, H., Feng, H., Xu, J. and Zhang, B., 2020. Quercetin radiosensitizes non-small cell lung cancer cells through the regulation of miR-16-5p/WEE1 axis. *IUBMB Life*, **72**: 1012-1022. <https://doi.org/10.1002/iub.2242>
- Wang, Y.R. and Du, E.Q., 2020. Expression levels and significance of miR-365, miR-135a-5p and STAT3 in cervical cancer tissues. *Chinese J. Woman Child Hlth. Res.*, **31**: 1065-1070.
- Xiong, R., Sun, X.X., Wu, H.R., Xu, G.W., Wang, G.X., Sun, X.H., Xu, M.Q. and Xie, M.R., 2020. Mechanism research of miR-34a regulates Axl in non-small-cell lung cancer with gefitinib-acquired resistance. *Thoracic Cancer*, **11**: 156-165. <https://doi.org/10.1111/1759-7714.13258>
- Yin, J., Hu, W., Pan, L., Fu, W., Dai, L., Jiang, Z., Zhang, F. and Zhao, J., 2019. Let 7 and miR 17 promote self-renewal and drive gefitinib resistance in non-small cell lung cancer. *Oncol. Rep.*, **42**: 495-508. <https://doi.org/10.3892/or.2019.7197>